BNL-77887-2007-BC

Pulse Radiolysis in Supercritical Rare Gas Fluids

Richard Holroyd

To be published in "Recent Trends in Radiation Chemistry"

April 2007

Chemistry Department

Brookhaven National Laboratory
P.O. Box 5000
Upton, NY 11973-5000
www.bnl.gov

DISCLAIMER

PULSE RADIOLYSIS IN SUPERCRITICAL RARE GAS FLUIDS

Richard Holroyd

Chemistry Department, Brookhaven National Laboratory, Upton, NY 11973, USA

INTRODUCTION

Recently, supercritical fluids have become quite popular in chemical and semiconductor industries for applications in chemical synthesis, extraction, separation processes, and surface cleaning.(1-3) These applications are based on: the high dissolving power due to density build-up around solute molecules, and the ability to tune the conditions of a supercritical fluid, such as density and temperature, that are most suitable for a particular reaction. The rare gases also possess these properties and have the added advantage of being supercritical at room temperature. Information about the density buildup around both charged and neutral species can be obtained from fundamental studies of volume changes in the reactions of charged species in supercritical fluids. Volume changes are much larger in supercritical fluids than in ordinary solvents because of their higher compressibility. Hopefully basic studies, such as discussed here, of the behavior of charged species in supercritical gases will provide information useful for the utilization of these solvents in industrial applications.

These studies require special cells to withstand the pressures involved, as well as radiation sources like high energy electrons or X-rays that will penetrate the necessarily thick windows or walls of the cell. Rare gases have the additional feature of high free ion yields that facilitate the study of ionic reactions. The high yield is a consequence of the

long time required to thermalize the electron; several nanoseconds are required since only elastic collisions are available for energy loss. During this time the electron travels well beyond the Onsager escape distance from the cation. The escape probability is therefore nearly 100%. The free ion yield, G, is around 5 ion-pairs/100 eV in xenon.(4,5) The yield is 5.4 in liquid krypton(6) and 4.1 for krypton gas.(7) There have been only a few pulse radiolysis studies carried out in dense xenon or krypton fluids. In the case of xenon this may be due in part to the high cost. However, since rare gases are radiation stable, they can be reused if additives from previous studies are removed.

This chapter focuses on the properties and reactions of charged species, electrons and ions in supercritical rare gases, as studied by pulse radiolysis. Intermediates have been detected either by their optical absorption or by conductivity. The transparency of the rare gases throughout the IR, visible and UV parts of the spectrum facilitates optical detection of intermediates, and the dielectric properties also permit DC conductivity measurements. Studies have been done in both xenon and krypton with picosecond resolution, which elucidate the early processes involving electron-ion recombination and excimer formation. Electron properties such as mobility and conduction band energy are reviewed because of their significance in the understanding of electron reactions. Partial molar volumes have been determined from studies of electron attachment reactions as a function of pressure. The properties and reactions of ions are also discussed. Mobility measurements have shown that ions have lower mobility than would be expected, which is attributed to clustering around the ions due to electrostriction. The clustering is also shown to affect the rate of charge transfer reactions in supercritical rare gases.

EARLY PROCESSES

Pulse-probe studies using the Laser Electron Accelerator Facility (LEAF)(8) at Brookhaven National Laboratory have revealed changes in optical absorption occurring on the picosecond time scale in rare gas fluids. In xenon, excimers are formed which absorb in the visible and near infra-red as shown in Fig. 1a. The absorption grows in during the first 50 picoseconds (see Fig. 1b).(9) This growth is concomitant with ion recombination that leads first to excited atoms, reaction 1a, which immediately form excimers, Xe_2^*, because of the high density of xenon.

$$e^- + Xe_2^+ \rightarrow Xe^* + Xe \qquad (1a)$$

$$Xe^* + Xe \rightarrow Xe_2^* \qquad (1b)$$

The observed fast formation of excimers in supercritical xenon, occurring in the first 50 ps, corresponds to a second order rate constant for reaction 1a of 7.5×10^{16} $M^{-1}s^{-1}$ at a density of 1.33 g/cm^3. This rate can be compared to the theoretical rate for electron-ion recombination as given by the reduced Debye Eq.:

$$k_r = 4\pi e (\mu_+ + \mu_-)/\epsilon = 1.09 \times 10^{15} (\mu_+ + \mu_-)/\epsilon \ M^{-1} s^{-1} \qquad (2)$$

where μ_+ and μ_- are the mobilities of the positive ion and electron, respectively in units of cm^2/Vs, and ϵ is the dielectric constant of the fluid. The mobility of the electron is many orders of magnitude larger than that of the ion, thus μ_+ can be ignored. The usual low-field mobility of the electron cannot be used in this case because the electrons are still 'hot' at picosecond times. The mobility of electrons at high electric fields, where the electrons are also 'hot', is between 60 to 100 cm^2/Vs.(10) The use of these values in Eq. 2 lead to a range for k_r from 5.0 to 8.4×10^{16} $M^{-1}s^{-1}$, consistent with the experimental value.

Two species of excimers are formed in xenon. One decays with a half-life of 5.4 ns, independent of pressure. This is identified as the singlet excimer. The other component is longer lived and the lifetime increases with decreasing pressure; this is identified as the triplet excimer.(9)

In supercritical krypton the formation of excimers has also been time resolved but the results contrast with those for xenon.(11) As in xenon, electron-ion recombination should occur rapidly. Again, electrons remain hot for many nanoseconds in krypton(12) and the mobility of hot electrons is in the range of 150 to 400 cm^2/Vs. This leads to a theoretical range for k_r of 1.4 to 3.6 x 10^{17} M^{-1},s^{-1} at a density of 0.48 g/cm^3. In pulse radiolysis studies using optical detection the concentration of intermediates is around 0.5 to 1 μM, thus recombination of electrons with ions should occur in less than 10 ps in krypton. What has been observed is that the singlet excimer, the spectrum of which is shown in Fig. 2a with peaks at 830, 890 and 990 nm, grows in over a period of a few nanoseconds (see Fig. 2b). Thus some of the vibrationally relaxed excimers are formed after a delay. Recombination leads first to a precursor, which then relaxes to the singlet excimer ($^1\Sigma_u^0$). At 113 bar the observed lifetime for relaxation is 1.9 nsec.(see Fig. 2b) It is suggested that the slow relaxation involves the excited excimer state ($^1\Sigma_g^+$).(13) The precursor cannot be the vibrationally excited excimer, ($^1\Sigma_u^*$) the relaxation of which should occur fast, at the collision rate; which at this pressure means within 10 psec. As is shown in Fig. 2b, there is significant absorption present immediately following the pulse. This could be due to the precursor but is also likely to be due to singlet excimers formed via the fast relaxation of excited excimers in the ungerade state($^1\Sigma_u^*$). Further mechanistic details can be found elsewhere.(11,13) At a pressure of 109 bar the singlet

decays with a lifetime of 3.4 ns and a new species is formed which absorbs at 1100 nm, (see Fig. 2a) identified as the triplet excimer ($^3\Sigma_u^0$), with a lifetime of 9 ns

Excitation Transfer. The rare gas excimers readily transfer energy to various additives. Rates for transfer to nitrogen and hydrogen in krypton are known at 1 atm.(14) Because excimer species have strong absorptions in the visible it is necessary to quench them when studying reactions of other intermediates by absorption spectroscopy. Ethane has been shown to be convenient for this purpose. The rate constant for excitation transfer from excimers to ethane in xenon was measured by the pulse-probe technique to be 3.4×10^{10} $molal^{-1}s^{-1}$ at pressures near 50 bar.(9) Thus, addition of a small concentration of ethane can be used to reduce the absorption due to excimers to a small level at nanosecond times.

IONIC PROPERTIES

Theory of Electrostriction. It is important to be aware of clustering caused by electrostriction in order to understand reactions of ions in supercritical rare gases. If a classical continuum model is used to calculate clustering, the magnitude of the volume change due to electrostriction would be overestimated because such a model ignores the density build-up around the ion. Because of this density augmentation the compressibility of the fluid near the ion is less and, since electrostriction is proportional to compressibility, the actual electrostriction will be less than predicted by a continuum model. A compressible continuum model was developed that takes clustering around the ion into account.(15,16) In this model the attraction between the ion and induced dipoles of solvent molecules is considered as a pressure. The local density is then calculated

from the pressure at each point using an equation of state. The local dielectric constant is calculated from this density. This process is iterated until the results converge. The volume change due to electrostriction, V_{el}, is then obtained by integrating over all space in the presence and absence of the ion.

In a similar way the polarization energy, P^-(CC), by the ions in a supercritical fluid can be calculated with this model taking into account the density dependence of the dielectric constant, which is enhanced as far out as 1 nm from the ion. Again integration over all space is involved and P^-(CC) obtained from the difference of the calculated energy of the ion in the supercritical fluid and the energy in vacuum. The magnitude of P^-(CC) calculated this way is generally larger than if the polarization energy is calculated using the Born continuum model. The compressible continuum model is used for estimation of the energetics of electron reactions (see below).

Experimental Evidence of Clustering. Evidence that clustering of rare gas atoms occurs around ions comes from: a) ion mobility measurements, and b) volume changes occurring on electron attachment to solutes. The mobility of positive ions in xenon decreases with increasing pressure and at pressures near 100 bar is 1.3×10^{-3} cm^2/Vs (see Fig. 3a) near room temperature.(10) An estimate of the size of the cluster moving with the ion may be obtained from such data using the Stokes equation,

$$R_{ion} = e/6\pi\eta\mu \qquad (3)$$

where η is the bulk value of the viscosity. This equation indicated clusters of about 0.6 nm at high pressure and much larger clusters in regions of high compressibility (see Fig. 3b). Eq. 3 is only an approximation since the high viscosity near an ion should be considered. This effect was taken into account in the hydrodynamic compressible

continuum model (HCC).(10) The HCC model also indicates the size of moving clusters to be 0.6 nm, or one complete solvation shell, in xenon at pressures above 75 bar, and nearer to 1 nm in regions of high compressibility.

Several studies have shown that clustering also occurs around negative ions in supercritical fluids. The mobility data for $C_6F_6^-$ in xenon (see Fig. 3a) indicate that the clusters around $C_6F_6^-$ are slightly smaller (see Fig. 3b) than those around the positive ion but the pressure dependence is similar.(9) Measurements of the mobility of O_2^- in argon at a temperature just above the critical temperature indicated the O_2^- ion also moves with a large solvation shell.(17)

Evidence of clustering is also obtained from studies of electron attachment reactions. These reactions occur in supercritical gases with large volume changes due to electrostriction around the negative ion formed. In supercritical ethane it has been shown that the compressible continuum model accurately predicts volume changes for reactions of electrons with CO_2,(16) pyrimidine(18) and pyrazine.(19) In xenon volume changes are smaller because of the significant clustering that occurs around neutrals, as discussed in the electron attachment/detachment section below.

ELECTRON PROPERTIES

Mobility. In order to understand the high rate of reaction of electrons in supercritical fluids one needs to know the electron mobility and how it changes with pressure. The electron mobility provides information on the diffusion constant since $D_e = \mu_e k_B T/e$ and values of D_e are necessary to calculate the rate of electron-ion recombination (see **EARLY PROCESSES**) and other diffusion controlled reactions (see **Electron**

Reactions). For supercritical xenon and krypton the electron mobility in the pressure range of interest is shown in Fig. 4. The mobility is generally high, from which it can be concluded that electrons are in a quasi-free state; that is, there are no trapped states. However, in xenon the mobility at 20 ^{o}C becomes unusually low near 60 bar as shown in Fig. 4. To explain this behavior of quasifree electrons, a modification of the Basak-Cohen model(20) has been invoked.(21) In this model the scattering of the electron is the result of density fluctuations resulting in a deformation potential. This potential is a function of derivatives of V_0, the conduction band energy, which is discussed in the next section. The model leads to Eq. 4 for the mobility:

$$\mu_e = \frac{2e\hbar^4\sqrt{2\pi}}{3m^{*5/2}(k_BT)^{1/2}n^2[V_0'^2\,k_BT\chi + (terms\,involving\,V_0'', V_0''')]} \qquad (4)$$

where m^* is the reduced mass of the electron and n is the density. The mobility is also a function of the compressibility, χ. In the original theory the isothermal compressibility was used, however it diverges near critical densities because density fluctuations become quite large. This results in a predicted near zero mobility in the vicinity of the critical density. It was suggested by many that electrons do not interact with large density fluctuations(22,23) and it was more appropriate to use the adiabatic compressibility. When the adiabatic compressibility (which changes smoothly with density) is used, Eq. (4) accounts for the pressure dependence of the mobility in xenon remarkably well as shown by the dashed line in Fig. 4.

The mobility in krypton is quite high at all pressures and there is only a shallow minimum in this case. The data shown in Fig. 4 are for 20 ^{o}C, which is well above the critical temperature. The minimum becomes lower at lower temperatures but not as low

as in xenon. The electron mobility in krypton is also reasonably well represented by Eq. 4 when the adiabatic compressibility is used.(12)

Conduction Band Energy. The energy of the electron in the conduction band in these fluids, measured from the vacuum level, is designated V_0. This energy term is important for several reasons. As shown in the previous section the electron mobility is a function of the derivatives of V_0. To first order the electron mobility depends inversely on $(dV_0/dn)^2$ Thus where the slope of the V_0 curve is steep as for xenon around 62 bar (see Fig. 5) the mobility is quite low (see Fig. 4). For krypton the slope of the V_0 curve is not as steep and consequently the mobility is higher in this pressure region. Also V_0 is important because the energy change for electron attachment/detachment reactions is a function of V_0 (see next section). As shown in Fig. 5, V_0 is negative at all pressures in both krypton and xenon because the interaction between electrons and atoms is positive. V_0 is quite low at higher pressures, which is consistent with the high values of the electron mobility observed. Generally trapping is unimportant for fluids with low V_0.

An early theoretical approach to calculate V_0 utilized the Wigner-Seitz model.(24) This model considered both the attractive polarization potential, including screening, and the repulsive kinetic energy of the impenetrable hard cores. There have been several modifications to the theory over the years using various techniques. A modification of the Wigner-Seitz model by Plenkiewicz, et al.(25) using an accurate pseudopotential gave reasonably good fits to experimental values of V_0 as a function of density. Recently Evans and Findley(26) reproduced their measurements of V_0 in krypton and argon to high precision using this model with an adjustable phase shift parameter.

The first measurements of V_0 in liquids utilized the change in work function of a metal when immersed in the liquid. Other techniques like photoionization have also been used. Recently a method utilizing the field ionization of a Rydberg state of an added solute has been applied to xenon and krypton.(26,27) The results for krypton shown in Fig. 5 were obtained by this method. Synchrotron radiation is used in this technique to excite the solute in the presence of an electric field. Photocurrents are measured at both high and low electric field. The field ionization spectrum is obtained by subtracting the spectrum at low field from one at high field. Such spectra show a peak near threshold due to the high-lying states that ionize at the high voltage but not at the low. The position of these peaks, E_{th}, shifts as the density or pressure changes depending on the value of V_0 and the polarization energy, P^+, of the positive ion of the solute according to:

$$E_{th} = IP + P^+ + V_0 \qquad (5)$$

In this technique determination of V_0 also requires calculation of the polarization energy of the positive core, P^+. The data in Fig. 5 are best fits to the experimental results obtained in recent studies.

ELECTRON REACTIONS

Electron Attachment. The reaction of electrons with a few solutes has been

$$e^- + O_2 \rightarrow O_2^- \qquad (6)$$

studied in xenon. In the case of oxygen the rate of attachment, k_a, is 2 x 10^{11} molal^{-1} s^{-1} at low pressure (see Fig. 6) and increases with increasing pressure overall by a factor of 5.(28) Most of the increase occurs in the region of high compressibility around 62 bar. Electron attachment to O_2 is a resonance process and the rate will depend on the energy

level of the electron in the fluid, V_0, and the polarization energy of the fluid by O_2^-. This reaction is quite exothermic; the free energy change is -1.8 eV at 100 bar in xenon (see Eq. 13 below). This mismatch in energy accounts for the slow rate.

The activation volume, V_a^*, for electron attachment to O_2 is calculated using Eq. 7:

$$V_a^* = -RT\,\partial(\ln k_1)/\partial P \qquad (7)$$

Values of V_a^* are generally small except near 62 bar where V_a^* reaches a minimum value of -9 L/mol. This is approximately one-third of that expected theoretically for electrostriction by O_2^-. Clearly there is a volume decrease in the reaction but the lack of agreement with theory indicates either that the full volume change is not obtained until the reaction is complete, or that O_2 has a significant cluster around it; i.e. the partial molar volume of neutral O_2 in xenon is negative.

The results for electron attachment to pyrazine as shown in Fig. 6 are similar to those for O_2 at low and high pressures; that is, the rate increases at low pressure and is fairly constant at high pressure. However around 62 bar, where the O_2 rate is increasing, the rate of attachment to pyrazine actually decreases slightly. The values of V_a^* derived from the data are negative at low pressures and generally quite small, but in contrast to O_2 exhibit a maximum of 3 L/mol at intermediate pressures. The explanation for this behavior lies in the significant role of clustering around the neutral pyrazine as explained under the electron attachment/detachment section below.

The rate constant for electron attachment to C_6F_6 in xenon is much larger than that

$$e^- + C_6F_6 \rightarrow C_6F_6^- \qquad (8)$$

of the other two solutes as shown in Fig. 6. The rate increases monotonically with pressure and shows a sharp increase at 62 bar.(9) The change in rate with pressure was originally interpreted as an activation volume, calculated using Eq. (7). This analysis showed that V_a* is small and negative except near 62 bar where a value of -28 L/mol was reported.(9) The value of -28 L/mol is coincidently close to the value expected for electrostriction calculated by the compressible continuum model, which is discussed above. However the change in rate with pressure should not have been attributed to a volume change because, as is shown in Fig. 6 the rate is clearly diffusion limited, at least at low and intermediate pressures. The diffusion rate is calculated from the mobility of the electron, μ_e, using:

$$k_D = 4\,\pi R \mu_e k_B T \rho N/\mathrm{e}1000 \text{ molal}^{-1}\ \mathrm{s}^{-1} \qquad (9)$$

The value of the radius, *R*, used is 1 nm, ρ is the density in g/cm^3. The value of the rate constant at high pressure is below the theoretical diffusion rate, however it is actually at or above the maximum value expected for electron attachment rates. Warman predicted that electron attachment rate constants are not expected to exceed 3 x 10^{14} M^{-1} s^{-1}.(29) That rate constant corresponds, in the units used in Fig. 6, to a value of 6 x 10^{14} molal^{-1} s^{-1} at the highest pressure; the observed rate is actually above this. Therefore deriving activation volumes from the C_6F_6 rate data is questionable.

Electron Attachment/Detachment. The reaction of the electron with pyrazine is reversible and the rate of electron detachment, k_d, from the pyrazine anion has been measured in supercritical xenon.(30)

$$\text{pyrazine}^- \leftrightarrows e^- + \text{pyrazine} \qquad (10)$$

When the values of k_d are combined with values of k_a (see Fig. 6) the free energy of reaction is obtained from: $\Delta G_r = -RT\ln(k_a/k_d)$. The change in ΔG_r with pressure provides information on the volume change in the reaction, since $\Delta V_r = (\partial \Delta G_r/\partial P)_T$. In xenon the free energy of reaction changes slowly with pressure and the derived volume changes are small, less than a few liters per mole. This is in contrast to the results obtained for electron attachment to pyrazine and methylpyrazine in supercritical ethane where ΔG_r decreases rapidly over very narrow pressure ranges which leads to volume changes ranging from -1 to -45 L/mol, depending on pressure and temperature. (19) Those volume changes were adequately accounted for by electrostriction of the ethane fluid around the pyrazine anion. Calculations of this effect using the compressible continuum model were in good agreement with the experimental values of ΔV_r. It was also concluded that in supercritical ethane the partial molar volume of the neutral pyrazine and methylpyrazine are small in magnitude, at least in comparison to that of the ions.

To explain the small volume changes observed for electron attachment to pyrazine in supercritical xenon, it was proposed that clustering around the neutral pyrazine is comparable to that around the ion.(30) The volume change in this reaction is given by:

$$\Delta V_r = \bar{V}(\mathrm{Pyz}^-) - \bar{V}(\mathrm{Pyz}), \qquad (11)$$

where the partial molar volume of the electron is presumed small. The partial molar volume of the neutral, $\bar{V}$ (Pyz), was calculated from experimental volume changes, ΔV_r, using this equation and $\bar{V}$ (Pyz^-), taken as the volume of electrostriction calculated by the compressible continuum model. At higher pressures $\bar{V}$ (Pyz) and $\bar{V}$ (Pyz^-) were comparable. Values of $\bar{V}$ (Pyz) thus obtained ranged from 0 to -9 L/mol and were

proportional to the compressibility as expected according to Eq. 12, where the coefficient *a* is negative.

$$\overline{V}\,(\mathrm{Pyz}) = a(T)\chi_T + b(T) \qquad (12)$$

Thus in xenon reaction (10) should be considered as electron attachment to a pyrazine molecule that already has a cluster of xenon atoms around it.

Energetics. In liquids the free energy change in electron attachment reactions is given by:(31,32)

$$\Delta G_r(\mathrm{liq}) = \Delta G_r(\mathrm{gas}) + P^- - \Delta G_s(e^-) \qquad (13)$$

where the polarization energy P^- is often approximated by the Born Eq. However, in supercritical fluids the Born Eq. does not work since it is a continuum model. In supercritical fluids there is considerable buildup of density around ions that affects this energy. The compressible continuum (CC) model works well and accounted for the free energy changes when reaction (10) was studied in supercritical ethane.(19) The CC model was also used to calculate the polarization energy for pyrazine ions in supercritical xenon. $\Delta G_s(e^-)$ is the free energy of solution of the electron and is approximated by V_0, which changes considerably with pressure as is shown in Fig. 5. If ΔG_r(gas) is approximated by – E.A., where E.A. is the electron affinity, Eq. (13) becomes:

$$\Delta G_r(\mathrm{liq}) = -\mathrm{E.A.} + P^-_{\mathrm{CC}} - V_0 \qquad (13a)$$

The electron affinity normally used is that of the molecule in the gas phase. But in this case the volume change information shows that the electron reacts with a clustered pyrazine molecule, $PyzXe_m$, and the electron affinity of the clustered species should be used. Since there was evidence that the electron affinity of the analogous species in argon, $PyzAr_m$ increased with *m* by a few tenths of an electron volt,(33) the measured

values of ΔG_r(liq) were used with Eq. (13a) along with calculated values of P^-_{CC} and V_0 to evaluate E.A. The results showed that the electron affinity of $PyzXe_m$ also increases by a few tenths of an electron volt as *m* increases.

CHARGE TRANSFER REACTIONS

Some electron transfer reactions have been studied in supercritical xenon. Two of them have been shown to be diffusion controlled and two are energy controlled. These reactions have been followed by changes in the optical absorption after the pulse. To carry out these studies requires that the rate of electron attachment to the solute be sufficiently fast to compete with ion recombination, which occurs on the picosecond time scale in pulse radiolysis. The solute hexafluorobenzene satisfies this criterion; the rate constant is sufficiently large (see Fig. 6) that millimolar concentrations will allow formation of anions. The rate constant for attachment to 4,4′-bipyridine (bipy) is also sufficiently large to satisfy this need.(28) Another requirement for making these studies is to quench the excimers whose optical absorptions are strong and can interfere with detection of ions. As mentioned under **Early Processes** a small concentration of ethane (0.4%) is sufficient for this purpose.

The rate constant for electron transfer from $C_6F_6^-$ to benzoquinone (BQ) reaction (14),

$$C_6F_6^- + BQ \rightarrow C_6F_6 + BQ^- \qquad (14)$$

shown by the points in Fig.7, was determined by the rate of decay of the 550 nm absorption of the hexafluorobenzene anion in the presence of benzoquinone.(9) The diffusion rate, shown by the solid line, was calculated from:

$$k_D = 4\pi(R_{ion} + R_{BQ})(D_{ion} + D_{BQ})\ \rho N/1000\ m^{-1}\ s^{-1} \qquad (15)$$

The values of R_{ion} and D_{ion} used in Eq. (15) were obtained from the mobility of the clustered anions. D_{ion}, calculated by the Einstein relation: $D_{ion} = \mu_{ion} k_B T/e$, follows the mobility of the ion, which is shown in Fig. 3a. For R_{BQ} the radius derived from the molar volume was used. D_{BQ} was derived from the radius using the Stokes-Einstein relation: $D_{BQ} = k_B T/6\pi\eta R_{BQ}$. The good agreement of the calculated line with the experimental results indicates the reaction is diffusion controlled. The peak in rate near 62 bar can be attributed to the peak in R_{ion} observed at this pressure, (see Fig. 3b) where the compressibility is a maximum. Very similar results were obtained for the reaction:(28)

$$bipy^- + BQ \rightarrow bipy + BQ^- \qquad (16)$$

This rate also shows a maximum in the same pressure region and is also diffusion limited.

Two other electron transfer reactions have been studied in xenon:

$$C_6F_6^- + O_2 \rightarrow C_6F_6 + O_2^- \qquad (17)$$

$$bipy^- + O_2 \rightarrow bipy + O_2^- \qquad (18)$$

The rates constants for these reactions vary little with pressure and are well below the calculated rate of diffusion. Both reactions are exothermic as can be demonstrated by taking the difference of the constituent half reactions. That is, for reaction (17) the free energy change is the difference between the free energy for attachment to O_2, reaction (6) and that for attachment to C_6F_6, reaction (8). Thus ΔG_r for reaction (17) should be given by:

$$\Delta G_r(17) = E.A.(C_6F_6) - E.A.(O_2) + P^-(O_2^-) - P^-(C_6F_6^-) \qquad (19)$$

A similar equation applies to reaction (18). Estimated values of ΔG_r for these reactions are given in Table 1.

Table 1. Energies and Rates of Charge Transfer

Reaction	Pressure (bar)	ΔG_r (eV)	Rate constant ($molal^{-1}$ s^{-1})
17	52	-0.68	1.0×10^{10}
17	75	-0.68	1.4×10^{10}
18	52	-0.86	1.6×10^{10}
18	75	-0.85	3.3×10^{10}

Both reactions are exothermic. Transfer from $bipy^-$ to O_2 is more favorable than transfer from $C_6F_6^-$ to O_2 and the rate is faster for the former reaction, (18), which is in agreement with the energy gap law of electron transfer.(34) Also the free energy does not change with pressure for these two reactions, which implies there are no overall volume changes in the reactions. This is as expected since clustering around the products should be very similar to that around the reactants.

CONCLUSION

Supercritical xenon and krypton are interesting solvents for the study of electron and ion reactions. The high free ion yields facilitate such studies. Clustering around ionic species must be recognized as it affects the mobility and diffusion of these species. The formation of excimers following ion-recombination has been elucidated by picosecond pulse-probe studies. The excimers readily transfer energy to added solutes like ethane. Electron attachment reactions can be fast because of the high mobility of electrons. Studies of the reversible electron attachment to pyrazine in xenon have shown

that significant clustering occurs around neutral species. The electron mobility is shown to be a function of the derivatives of the conduction band energy. The conduction band energy also is important in understanding the energetics of electron reactions.

ACKNOWLEDGEMENT

This research was carried out at Brookhaven National Laboratory under contract DE-AC02-98-CH10886 with U.S. Department of Energy and supported by its Division of Chemical Sciences, Biosciences and Geosciences, Office of Basic Energy Sciences.

FIGURE LEGENDS

Fig. 1a. Spectra of excimers in xenon at 79 bar.

Fig. 1b. Growth of excimer spectra at 800 nm in xenon at 67 bar.

Fig. 2a. Spectra of excimers in krypton at 110 bar. Solid line: spectra of singlet at 2 ns after pulse; dotted line: spectra of triplet at 9 ns.

Fig. 2b. Growth and decay of singlet excimer in krypton at 113 bar recorded at 920 nm. Solid line is fit.

Fig. 3a. Mobility of ions in Xe versus pressure. Solid line: Xe_2^+, dotted line: $C_6F_6^-$.

Fig. 3b. Radii of ions in Xe versus pressure calculated using the Stokes' Eq. 3: ● Xe_2^+, ○ $C_6F_6^-$.

Fig. 4 Electron mobility in ● Xe and ■ Kr at 293 K versus pressure. Dashed line is theory for Xe, Eq. 4, using the adiabatic compressibility.

Fig. 5 Conduction band energy in ● Xe and ■ Kr versus pressure at 293 K (from Refs(26,27)).

Fig. 6 Rate constants for electron attachment versus pressure. ○ O_2; □ pyrazine; Δ C_6F_6; dotted line: calculated rate of diffusion.

Fig. 7 Rate constant for electron transfer from $C_6F_6^-$ to benzoquinone versus pressure. Points are experimental; the solid line is from Eq. 15 using the cluster radii for $C_6F_6^-$ calculated with Stokes' Eq. (3).

REFERENCES

(1) Eckert, C.A.; Knutson, B.L.; Debenedetti, P.G. (1996**)** Supercritical fluids as solvents... *Nature*, ***383***, 313-318.

(2) Savage, P.E.; Gopalan, S.; Mizan, T.I.; Martino, C.J.; Brock, E.E. (1995**)** Reactions at supercritical conditions... *AIChE Journal*, ***41***, 1723-1778.

(3) Kern, W. *Handbook of Semiconductor Wafer Cleaning Technology*; William Andrew Publishing: NY, 1993.

(4) Bolotnikov, A.; Ramsey, B. (1997**)** The spectroscopic properties of high-pressure xenon**.** *NIM A*, ***396***, 360-370.

(5) Srdoc, D.; Inokuti, M.; Krajcar-Bronic, I. "Atomic and Molecular Data for Radiotherapy and Radiation Research," 1995.

(6) Aprile, E.; Bolotnikov, A.; Chen, D.; Mukherjee, R. (1993**)** W value in liquid krypton**.** *Phys. Rev A*, ***48***, 1313-1318.

(7) Combecher, D. (1980**)** Measurement of W Values of low energy electrons in several gases**.** *Radiation Research*, ***84***, 189-218.

(8) Wishart, J.F.; Cook, A.R.; Miller, J.R. (2004**)** The LEAF Picosecond Pulse Radiolysis Facility at Brookhaven National Laboratory**.** *Rev. Sci. Inst.*, ***75***, 4359 - 4366.

(9) Holroyd, R.A.; Wishart, J.F.; Nishikawa, M.; Itoh, K. (2003**)** Reactions of Charged Species in Supercritical Xenon as Studied by Pulse Radiolysis**.** *J. Phys. Chem. B*, ***107***, 7281-7287.

(10) Itoh, K.; Holroyd, R.A.; Nishikawa, M. (2001**)** Ion mobilities in supercritical ethane, xenon, and carbon dioxide**.** *J. Phys. Chem. A*, ***105***, 703-709.

(11) Holroyd, R.A.; Preses, J.M., Pulse Radiolysis of Krypton using Picosecond Electron Pulses.

(12) Nishikawa, M.; Holroyd, R.A. Mobility of electrons in supercritical Kr; role of density fluctuations**.**

(13) Janssens, H.; Vanmarcke, M.; Desoppere, E.; Lenaerts, J.; Boucique, R.; Wieme, W. (1987**)** A general consistent model for formation and decay of rare gas excimers in the 10^{-2}-10^{+5} mbar pressure range, with application to krypton**.** *J. Chem. Phys.*, ***86***, 4925-4934.

(14) Ito, Y.; Arai, S. (1984**)** Kinetic Study of Excited Diatomic Molecules of Krypton and Xenon**.** *Bull. Chem. Soc. Jpn.*, ***57***, 3062-3065.

(15) Nishikawa, M.; Holroyd, R.; Itoh, K. (1998**)** Electron attachment to NO in supercritical ethane**.** *J. Phys. Chem. B*, ***102***, 4189-4192.

(16) Nishikawa, M.; Itoh, K.; Holroyd, R.A. (1999**)** Electron attachment to CO_2 in supercritical ethane**.** *J. Phys. Chem. A*, ***103***, 550-556.

(17) Borghesani, A.F.; Neri, D.; Barbarotto, A. (1997**)** Mobility of O_2^- ions in near critical Ar gas**.** *Chem. Phys. Lett.*, ***267***, 116-122.

(18) Holroyd, R.A.; Nishikawa, M.; Itoh, K. (1999**)** Thermodynamics of electron attachment to pyrimidine and styrene in supercritical ethane**.** *J. Phys. Chem. B*, ***103***, 9205-9210.

(19) Holroyd, R.A.; Nishikawa, M.; Itoh, K. (2000**)** Solvent clustering around pyrazine ions in the high-compressibility region of supercritical ethane**.** *J. Phys. Chem. B*, ***104***, 11585-11590.

(20) Basak, S.; Cohen, M.H. (1979**)** Deformation-potential theory for the mobility of excess electrons in liquid argon**.** *Phys. Rev. B,* ***20***, 3404-3414.
(21) Holroyd, R.A.; Itoh, K.; Nishikawa, M. (2003**)** Density inhomogeneities and electron mobility in supercritical xenon**.** *J. Chem. Phys.*, ***118***, 706-710.
(22) Steinberger, I.T.; Zeitak, R. (1986**)** Estimation of electron mobilities near the critical point in simple nonpolar fluids**.** *Phys . Rev. B,* ***34***, 3471-3474.
(23) Nishikawa, M. (1985**)** Electron mobility in fluid argon: application of a deformation potential theory**.** *Chem. Phys. Lett.*, ***114***, 271-273.
(24) Springett, B.E.; Jortner, J.; Cohen, M.H. (1968**)** Stability criterion for the localization of an excess electron in a nonpolar fluid**.** *J. Chem. Phys.*, ***48***, 2720-2731.
(25) Plenkiewicz, B.; Frongillo, Y.; Lopez-Castillo, J.-M.; Jay-Gerin, J.-P. (1996**)** A simple but accurate "core-tail" pseudopotential approach to the calculation of the conduction-band energy V_0 of quasifree excess electrons and positrons in nonpolar fluids**.** *J. Chem. Phys.*, ***104***, 9053-9057.
(26) Evans, C.M.; Findley, G.L. (2005**)** Energy of the Quasifree Electron in Argon and Krypton**.** *Phys . Rev.*, ***A72***, 022717.
(27) Altmann, K.N.; Reininger, R. (1997**)** Density dependence of the conduction-band minimum in fluid krypton and xenon from field ionization of $(CH_3)_2S$**.** *J. Chem. Phys.*, ***107***, 1759-1764.
(28) Holroyd, R.A.; Nishikawa, M.; Itoh, K. (2005**)** Rates and Energy of Reactions of Charged Species in Supercritical Xenon**.** *Radiat. Phys. Chem.*, ***74***, 146-151.
(29) Warman, J.M. In *The Study of Fast Processes and Transient Species by Electron Pulse Radiolysis*; Baxendale, J. H., Busi, F., Eds.; Reidel: Dordrecht, Holland, 1982, p 433ff.
(30) Holroyd, R.A.; Preses, J.M.; Nishikawa, M.; Itoh, K. (2007**)** Energetics and Volume Changes in Electron Attachment to Pyrazine in Supercritical Xenon**.** *J. Phys Chem.*
(31) Holroyd, R.A.; Nishikawa, M. (2002**)** Pressure effects on electron reactions and mobility in nonpolar liquids**.** *Radiat. Phys. Chem.*, ***64***, 19-28.
(32) Holroyd, R.; Itoh, K.; Nishikawa, M. (1997**)** Studies of $e^- + CO_2 = CO_2^-$ equilibria... *Chemical Physics Letters*, ***266***, 227-232.
(33) Song, J.K.; Lee, N.K.; Kim, S.K. (2002**)** Photoelectron spectroscopy of pyrazine anion clusters**.** *J. Chem. Phys.*, ***117***, 1589-1594.
(34) Tachiya, M. (1993**)** Generalization of the Marcus Equation for the Electron-Transfer Rate**.** *J. Phys. Chem.*, ***97***, 5911-5916.

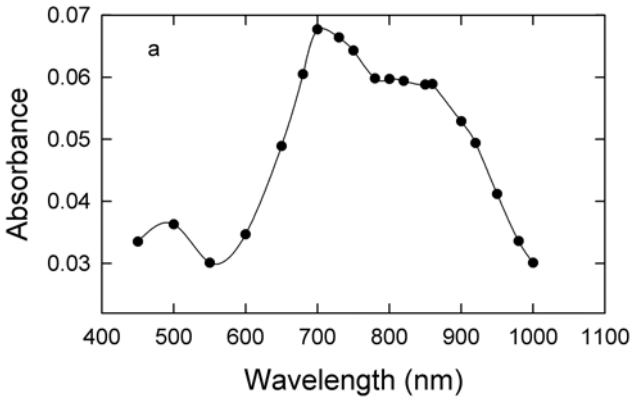

Fig. 1a. Spectra of excimers in xenon at 79 bar.

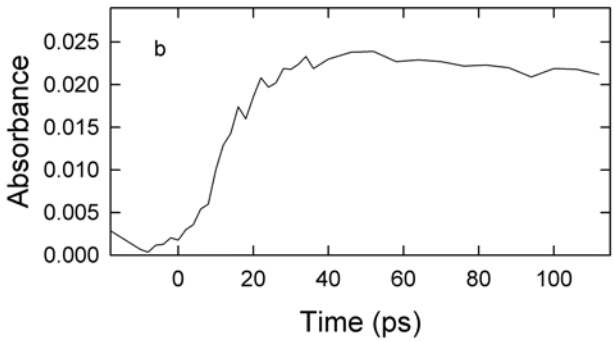

Fig. 1b. Growth of excimer spectra at 800 nm in xenon at 67 bar.

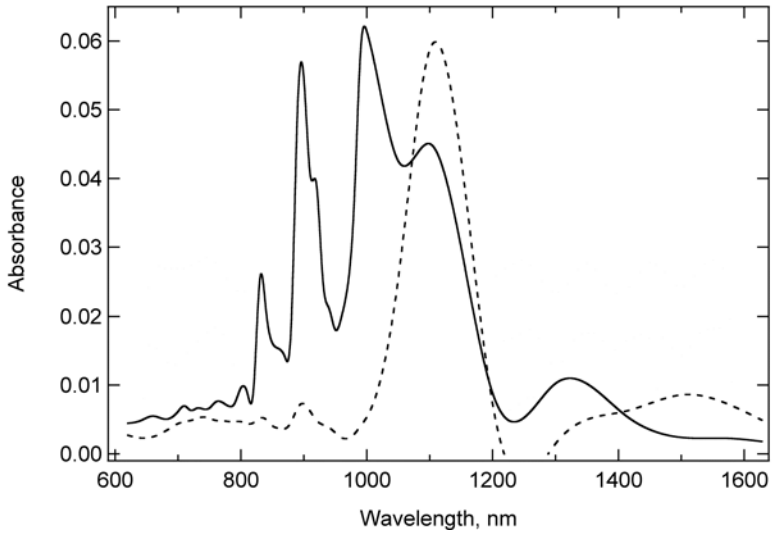

Fig. 2a. Spectra of excimers in krypton at 110 bar. Solid line: spectra of singlet at 2 ns after pulse; dotted line: spectra of triplet at 9 ns.

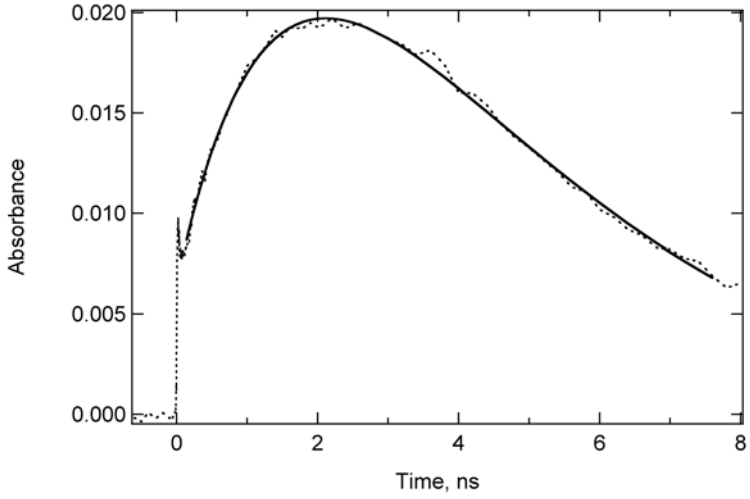

Fig. 2b. Growth and decay of singlet excimer in krypton at 113 bar recorded at 920 nm. Solid line is fit.

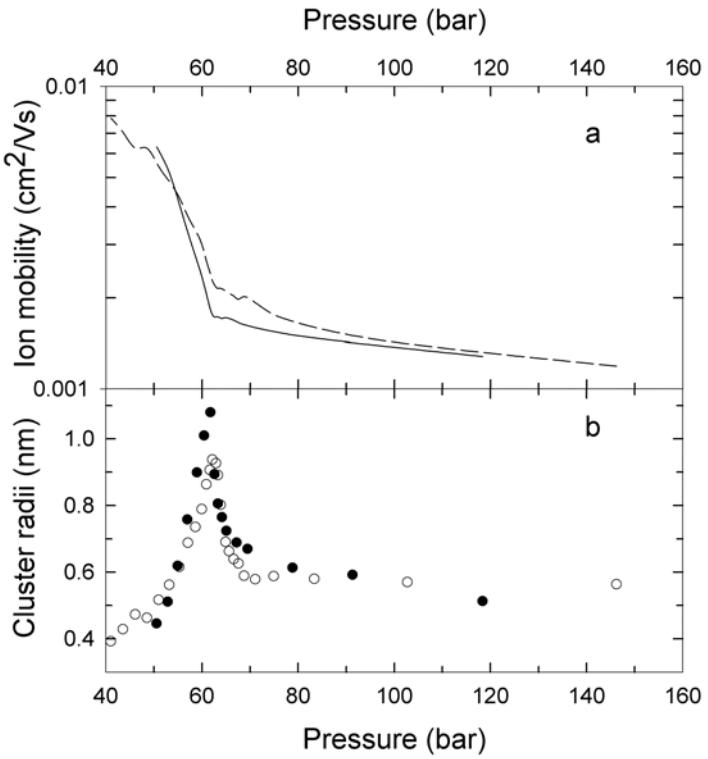

Fig. 3a. Mobility of ions in Xe versus pressure. Solid line: Xe_2^+, dotted line: $C_6F_6^-$.

Fig. 3b. Radii of ions in Xe versus pressure calculated using the Stokes' Eq. 3: ● Xe_2^+, ○ $C_6F_6^-$.

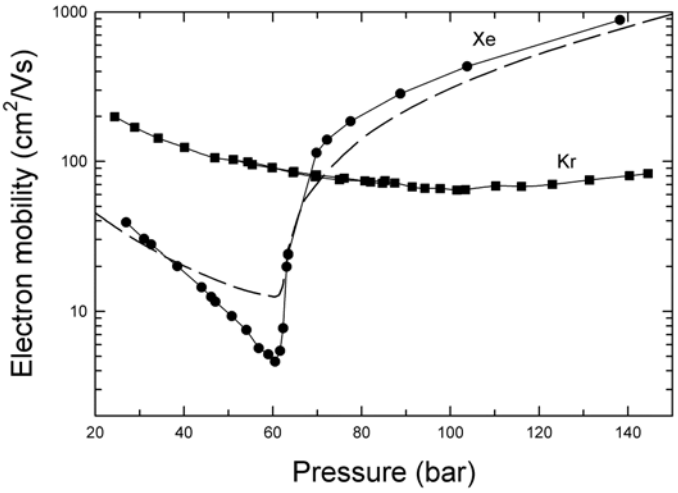

Fig. 4 Electron mobility in ● Xe and ■ Kr at 293 K versus pressure. Dashed line is theory for Xe, Eq. 4, using the adiabatic compressibility.

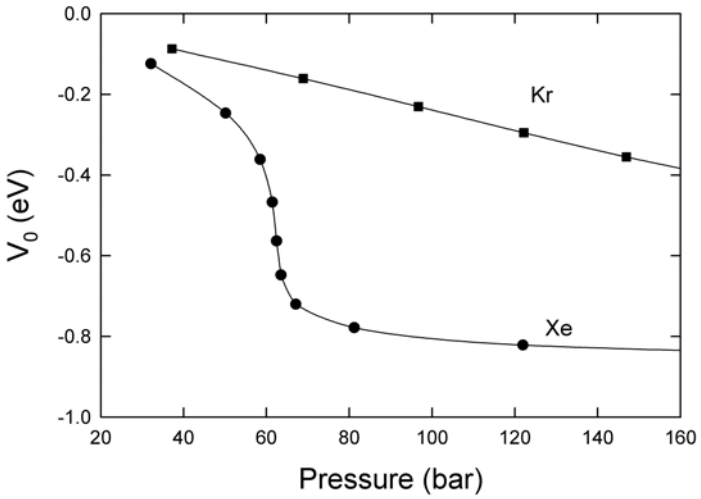

Fig. 5 Conduction band energy in ● Xe and ■ Kr versus pressure at 293 K (from Refs(26,27)).

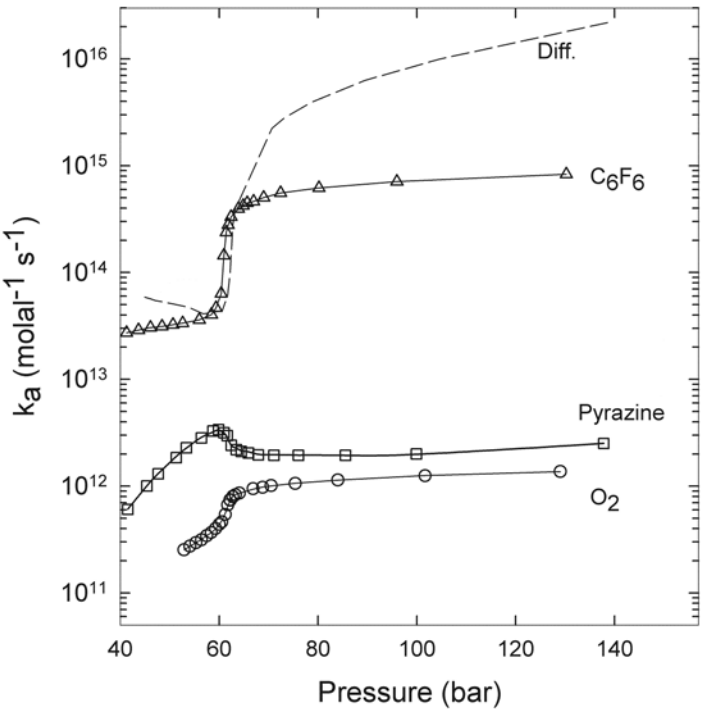

Fig. 6 Rate constants for electron attachment versus pressure. ○ O_2; □ pyrazine; Δ C_6F_6; dotted line: calculated rate of diffusion.

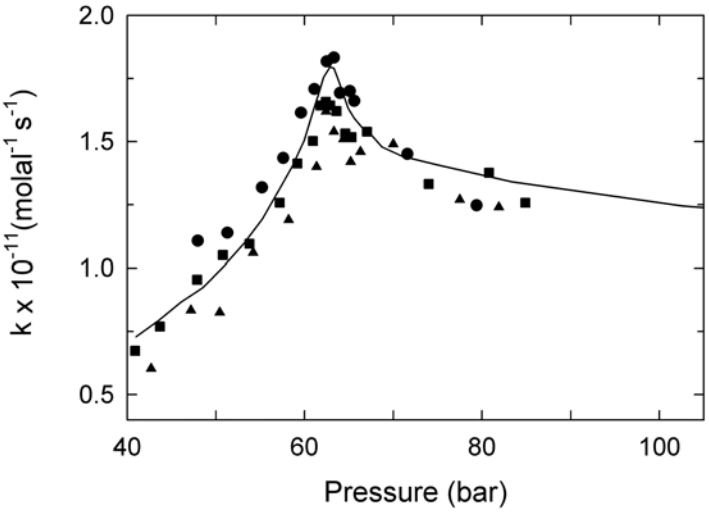

Fig. 7 Rate constant for electron transfer from $C_6F_6^-$ to benzoquinone versus pressure. Points are experimental; the solid line is from Eq. 15 using the cluster radii for $C_6F_6^-$ calculated with Stokes' Eq. (3).